Available online at www.sciencedirect.com
ScienceDirect
Physics Letters A 366 (2007) 397–402
PHYSICS LETTERS A
www.elsevier.com/locate/pla

A simple chaotic delay differential equation

J.C. Sprott *

Department of Physics, University of Wisconsin–Madison, Madison, WI 53706, USA

Received 21 November 2006; received in revised form 16 January 2007; accepted 18 January 2007

Available online 21 February 2007

Communicated by C.R. Doering

Abstract

The simplest chaotic delay differential equation with a sinusoidal nonlinearity is described, including the route to chaos, Lyapunov exponent spectrum, and chaotic diffusion. It is prototypical of many other high-dimensional chaotic systems.

PACS: 02.30.Ks; 02.30.Oz; 05.45.-a; 05.45.Jn; 05.45.Pq

Keywords: Chaos; Lyapunov exponent; Delay differential equation; Brownian motion

1. Introduction

There has been much recent interest in identifying the algebraically simplest examples of continuous-time systems that exhibit chaos. For example, the simplest dissipative chaotic flow with a single quadratic nonlinearity is [1]

$$\dddot{x} + a\ddot{x} - \dot{x}^2 + x = 0 \tag{1}$$

where $\dot{x} = dx/dt$, for which chaos occurs over most of the range $2.0168 < a < 2.0577$. The simplest periodically-driven chaotic conservative flow with a cubic nonlinearity is [2]

$$\ddot{x} + x^3 = \sin \Omega t \tag{2}$$

which is chaotic over most of the range $0 < \Omega < 2.8$ and has its maximum Lyapunov exponent of 0.0971 at $\Omega \cong 1.88$. For high-dimensional systems of ordinary differential equations (ODEs), a particularly simple and elegant example is [3]

$$\dot{x}_i = \sin x_{1+i \bmod N} \tag{3}$$

which is chaotic for all $N \geqslant 3$ for most initial conditions. Other minimal examples include 3D ODEs with cubic [4] and absolute-value [5] nonlinearities, 3D [6] and 4D [7] Lotka–Volterra models, 4D hyperchaotic systems [8], and infinite-dimensional Lotka–Volterra models [9].

This Letter addresses the occurrence of chaos in the arguably simplest example of a delay differential equation (DDE) [10]. It is of a special type more properly called a retarded delay differential equation (RDDE) or a retarded functional differential equation (RFDE), in which the past dependence is through the single real state variable rather than through its derivatives. In addition, the dependence will be autonomous (not explicitly involving time) and will involve the value of the state variable at a single discrete time lag. DDEs have been used extensively to model population dynamics [11] with their inherent maturation and gestation time delays, but also to study epidemics [12], tumor growth [13], immune systems [14], lossless electrical transmission lines [15], and the electrodynamics of interacting charged particles (the Lorenz force with Liénard–Weichert potentials) [16], among others.

A standard and much studied DDE is the Mackey–Glass equation [17–19], proposed to model the production of white blood cells and given by

$$\dot{x} = \frac{ax_\tau}{1 + x_\tau^c} - bx \tag{4}$$

where $x_\tau = x(t - \tau)$ is the value of x at an earlier time of $t - \tau$ for which chaos occurs with parameters such as $a = 0.2$, $b = 0.1$, $c = 10$, and $\tau = 23$. Another example is the Ikeda DDE [20], proposed to model a passive optical bistable res-

* Fax: +1 608 2627205.
E-mail address: sprott@physics.wisc.edu.

0375-9601/$ – see front matter
doi:10.1016/j.physleta.2007.01.083

onator system [21] and given by

$$\dot{x} = \mu \sin(x_\tau - x_0) - x. \tag{5}$$

While there are values of the parameters such as $\mu = 20$, $x_0 = \pi/4$, and $\tau = 5$ that give chaos, this is not the simplest such system since chaos also occurs in the one-parameter system

$$\dot{x} = \sin x_\tau \tag{6}$$

which is surely the simplest DDE with a sinusoidal nonlinearity and whose dynamics will constitute the remainder of this Letter.

2. Route to chaos

For the case of no time delay ($\tau = 0$), Eq. (6) becomes $\dot{x} = \sin x$ with equilibria at $x^* = m\pi$, where m is an integer. The equilibria with m even are unstable with eigenvalues $\lambda = 1$, while those with m odd are stable with eigenvalues $\lambda = -1$. The equation can be integrated to calculate the approach to the stable equilibrium closest to the starting point, giving $x(t) = 2\tan^{-1}\{e^t \tan[x(0)/2]\}$, where $x(0)$ is the initial value of x at $t = 0$.

The stable equilibrium can be moved to the origin by placing a minus sign in front of the $\sin x$ term in Eq. (6), but the results that follow are otherwise unchanged. Similarly, the $\sin x$ term can be replaced with $\cos x$, moving the equilibria to $x^* = m\pi/2$ with m odd, without otherwise changing the behavior. Note also that by a trivial rescaling of $t = T/\tau$, Eq. (6) can be rewritten as $dx/dT = \tau \sin x(T - 1)$.

For $\tau > 0$ the system is infinite-dimensional in the sense that infinitely many initial conditions over the continuous range $-\tau < t < 0$ are required, and the system can be approximated by an infinite-dimensional system of ODEs such as

$$\begin{aligned} \dot{x}_0 &= \sin x_N, \\ \dot{x}_i &= N(x_{i-1} - x_i)/\tau, \end{aligned} \tag{7}$$

where $1 \leqslant i \leqslant N \to \infty$. The second equation above advances N discrete time lags of x_0 over the interval $t - \tau$ to t. For computational purposes, Eq. (7) can be simply solved by the Euler method

$$\begin{aligned} x_0(t + h) &= x_0(t) + h \sin x_N, \\ x_i(t + h) &= x_{i-1}(t), \end{aligned} \tag{8}$$

where $h = \tau/(N + 1/2)$. The factor of $N + 1/2$ comes from the fact that the Euler method already has a delay of $\tau = h/2$ even for $N = 0$ because it uses the value of x_N at time t rather than at the midpoint between t and $t + h$, which would provide a more accurate solution.

Normally a discrete-time Euler approximation would be less accurate than a continuous-time ODE, but in this case, it more accurately approximates the DDE for a given N since the iterates of Eq. (8) for $i > 0$ exactly give the previous N values of x_0. This method works well for Eq. (7) because its right-hand side does not involve $x(t)$. Said differently, any ODE solved by the Euler method using a step size of h is actually a DDE with $\tau = h/2$.

The eigenvalues for the flow in the vicinity of the stable equilibrium for $N \to \infty$ are given by the solutions of $e^{-\lambda\tau} + \lambda = 0$, which can be expressed in terms of the Lambert function [22] W as $\lambda = W(-\tau)/\tau$. This equation has two real roots for $\tau < 0.36787944\ldots$, and they are the two largest Lyapunov exponents [23]. At that value of τ, the equilibrium switches from a stable node to a stable focus with infinitely many complex eigenvalues. When τ reaches $\pi/2$, two of the eigenvalues are $\lambda = \pm i$, and a Hopf bifurcation occurs, giving rise to a limit cycle with a period of 2π. The system has $N + 1$ Lyapunov exponents whose sum for $\tau < \pi/2$ is $-(N/\tau)\log(N/\tau)$. As N approaches infinity, the system is infinitely dissipative with nearly all directions attracting, and nearly all eigenvalues are complex conjugate pairs.

For τ slightly greater than $\pi/2$, the stable limit-cycle oscillation with a period $\sim 4\tau$ has an amplitude of $\delta x \cong (\pi/2)\sqrt{2\tau - \pi}$, which grows in size with increasing τ while developing significant third and higher odd harmonics (period $4\tau/3, 4\tau/5, \ldots$), until the waveform $x(t)$ becomes almost triangular at $\tau \sim 3$. At $\tau \cong 3.894$ a pitchfork bifurcation occurs beyond which there are two coexisting stable limit cycles that mirror one another with even harmonics (period $\tau/2$, $\tau/4$, $\tau/6, \ldots$), each with a broken up-down symmetry of the waveform $x(t)$. These limit cycles continue to grow until a period-doubling occurs at $\tau \cong 4.828$. The period-2 limit cycles persist until $\tau \cong 4.978$, whereupon they alternate with period-12 limit cycles in a period sextupling bifurcation, finally giving way to chaos at $\tau \cong 4.991$ when the amplitudes of the limit cycles reach $\pm\pi$.

The onset of chaos coincides with an attractor-merging crisis in which the trajectory is suddenly able to access the entire region $-\infty < x < +\infty$. Chaos persists for most values of $\tau > 5$ except for a (possibly infinite) number of periodic windows, the most prominent of which is a period-2 limit cycle that onsets in a saddle-node bifurcation at $\tau \cong 5.535$. This limit cycle continues a period-doubling cascade at $\tau \cong 5.581$, culminating in chaos at the accumulation point of $\tau \cong 5.603$, with a similarity factor of about 5.0 ± 0.5 in agreement with the Feigenbaum constant of $\delta = 4.669201\ldots$ for unimodal maps [24].

For yet larger values of τ, the periodic windows become increasingly less evident, although there are values such as $12.23 < \tau < 14.68$ where the chaotic attractor coexists with a thin 2-torus. In this region, the resulting attractor depends on the initial conditions and on whether the region is approached from the large or small τ direction, and the bifurcation points exhibit hysteresis and long transients. For values of $\tau > 14.68$, no further periodic windows or coexisting attractors are evident, and chaos is generic.

All of these details are summarized in Table 1 and in Figs. 1–3. Fig. 1 shows the spectrum of Lyapunov exponents (using the Wolf algorithm) [25], the Kaplan–Yorke dimension [26], the Kolmogorov–Sinai entropy (the sum of the positive Lyapunov exponents) [27], and the bifurcation diagram (local maxima of $x \bmod 2\pi$) versus τ for $N = 100$. These plots were obtained by slowly increasing τ without resetting the initial conditions and calculating for a time of $t = 1990\tau$ (2×10^5 iterations) at each τ. Fig. 2 shows the attractor in

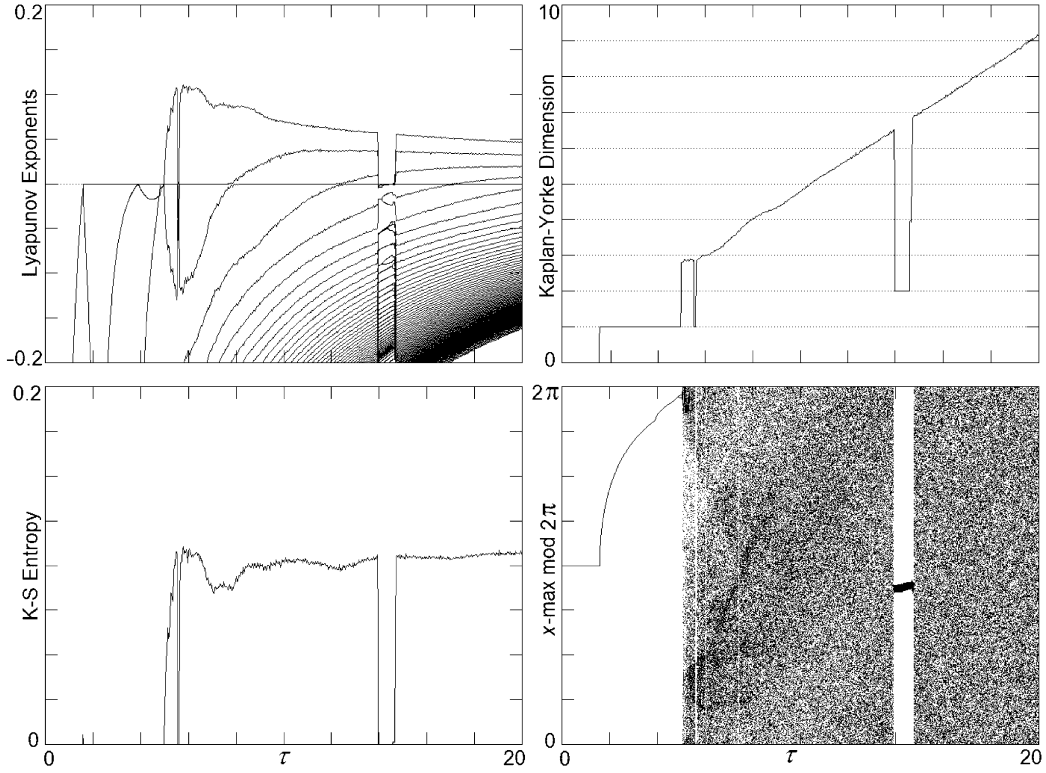

Fig. 1. Variation of Lyapunov exponents, Kaplan–Yorke dimension, Kolmogorov–Sinai entropy, and local maximum of x with time delay τ.

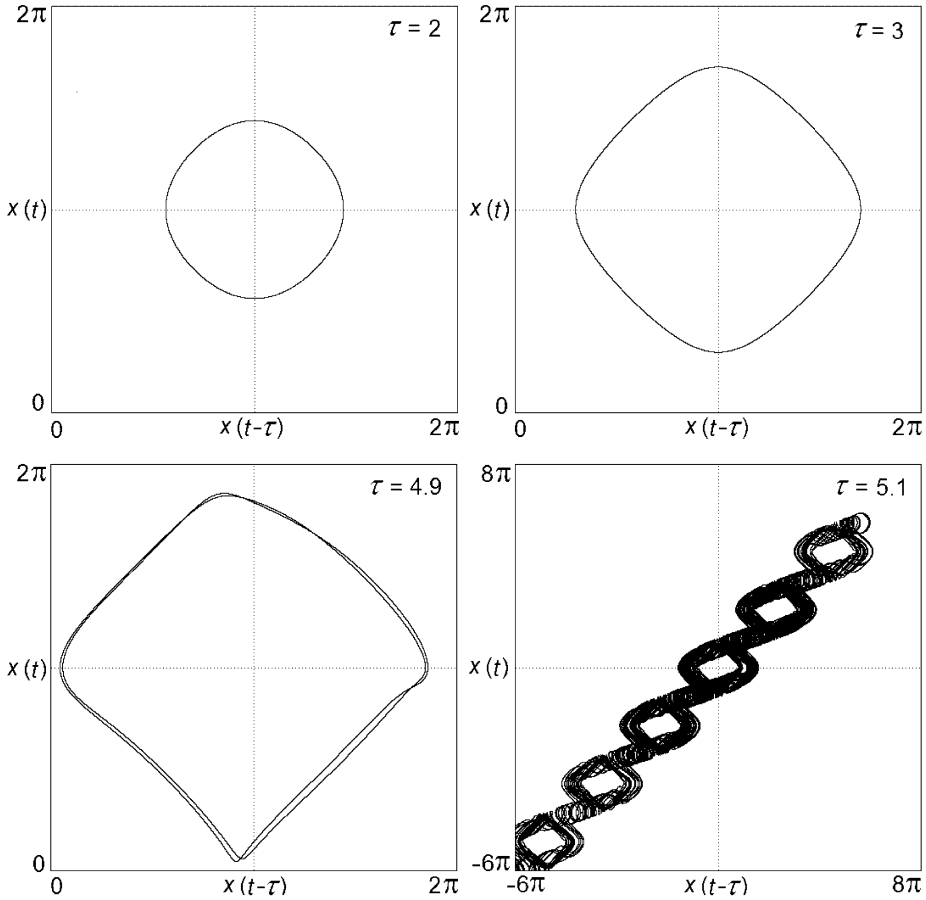

Fig. 2. Plots of $x(t)$ versus $x(t-\tau)$ for increasing τ showing the growth of the limit cycle, period doubling, and the onset of chaos at $\tau \cong 5$.

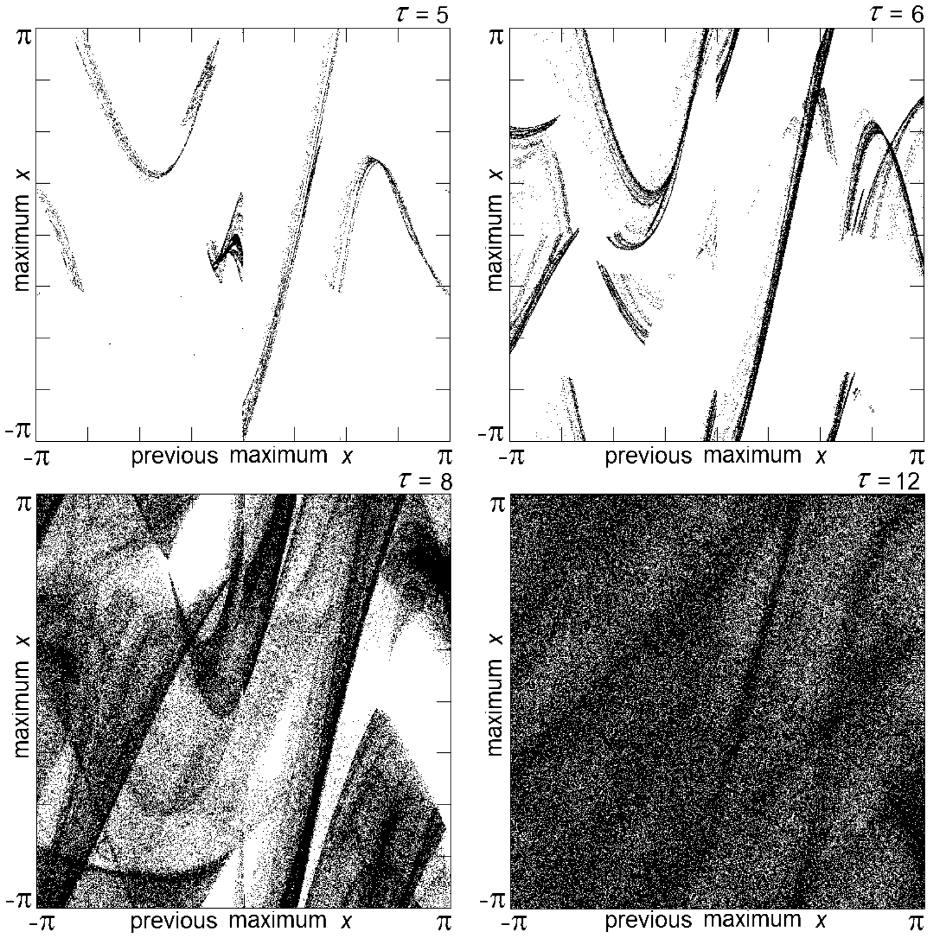

Fig. 3. Return maps (modulo 2π) for increasing τ showing the increasing complexity of the attractor beyond the onset of chaos at $\tau \cong 5$.

Table 1
Route to chaos in Eq. (6)

τ	Dynamic
	Stable equilibrium
1.571	Hopf bifurcation
	Limit cycle
3.894	Pitchfork bifurcation
	Limit cycles
4.828	Period-doubling bifurcation
	Period-2 limit cycles
4.978	Period-sextupling bifurcation
	Alternating 2-cycle and 12-cycle
4.991	Attractor-merging crisis
	Chaos
5.535	Saddle-node bifurcation
	Period-2 limit cycle
5.581	Period-doubling bifurcation
	Period-doubling cascade
5.603	Accumulation point
	Chaos

$x - x_\tau$ space for four different values of τ with $N = 6000$, and Fig. 3 shows return maps (modulo 2π) for the local maxima of $x(t)$ versus the previous local maximum for four different values of τ with $N = 6000$. The bifurcations and other behavior are indistinguishable for $N = 100$ and $N = 6000$, allaying any concern that the results are an artifact of the numerical method.

A linear regression to the Kaplan–Yorke dimension in the chaotic region (where $D_{KY} > 3$) gives $D_{KY} = 0.437\tau + 0.406$ for $\tau \leqslant 40$. The KS entropy is relatively constant with a value of about 0.1, indicating that the rate of creation of new information (or loss of information about the initial condition) is nearly independent of τ as one might expect. Similar behavior is observed in the Mackey–Glass and Ikeda DDE and may be a general feature of DDEs. All of the Lyapunov exponents approach zero as τ increases. Note that there are $N + 1$ exponents in the calculated map even though the actual DDE has infinitely many exponents. When the calculation for $N = 100$ is repeated with $N = 200$, the largest 101 of the exponents are nearly identical, and the additional 100 are more negative than the most negative for $N = 100$, although the spacing between the additional exponents becomes ever smaller as N increases. A linear regression to the number of positive Lyapunov exponents in the chaotic region (where $D_{KY} > 3$) gives $N_{PE} = 0.211\tau - 0.359$ for $\tau \leqslant 40$, with hyperchaos ($N_{PE} \geqslant 2$) for $\tau > 7.8$.

3. Deterministic Brownian motion

In the chaotic regime, $x(t)$ can take on any value, but only by executing a one-dimension deterministic Brownian motion

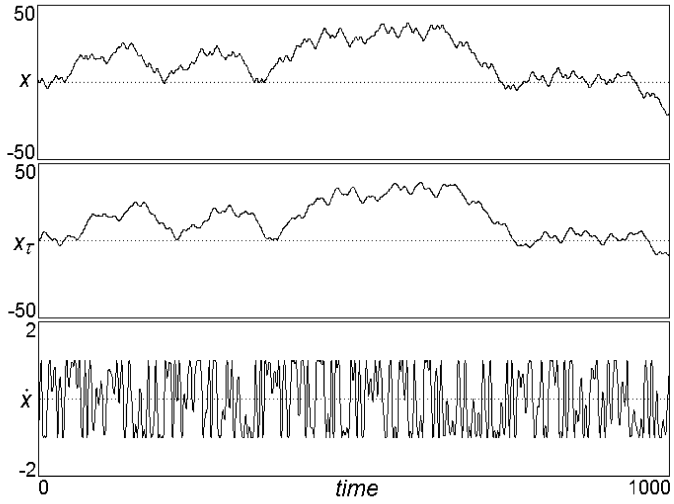

Fig. 4. Time history of x, x_τ, and dx/dt for $\tau = 20$ showing Brownian motion.

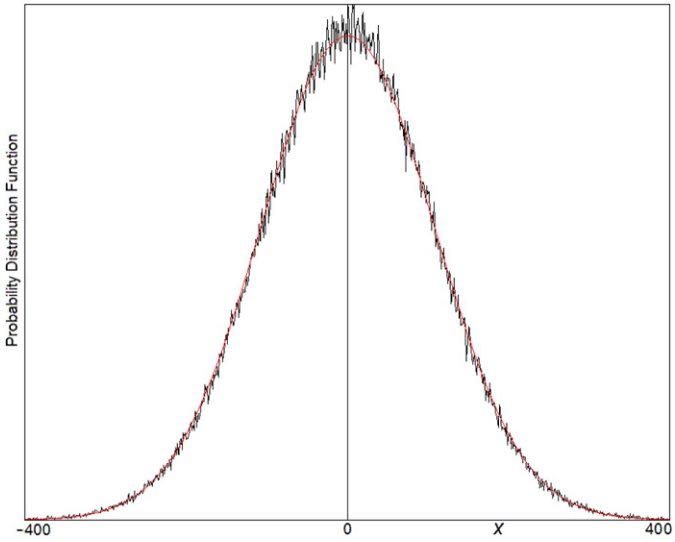

Fig. 5. (Colour online.) Probability distribution function of x for 5×10^5 initial conditions near the origin after a time of 4×10^3 with $\tau = 20$. The red curve is a Gaussian distribution with the same standard deviation and area.

as shown in Fig. 4 for $\tau = 20$ and $N = 100$. For a collection of 5×10^5 initial conditions that start at random positions near the origin (uniform over the range $-0.1 < x_i(0) < 0.1$), the probability distribution function along the x-axis after a time lapse of 4×10^3 is shown in Fig. 5 for $\tau = 20$ and $N = 100$. Also shown in the figure in red is a Gaussian distribution with the same standard deviation ($\sigma \cong 107.5$) and area. The observed distribution is nearly Gaussian with a negligible kurtosis [28] of $k \cong 0.125$. The kurtosis is defined such that a value of $k = 0$ represents a normal (Gaussian) distribution, and the calculated small positive value indicates that the distribution is very slightly leptokurtic (the tail of the distribution is slightly enhanced relative to a Gaussian). The standard deviation and kurtosis do not depend strongly on τ for τ approximately 20 or greater at a fixed time (data not shown).

The standard deviation of this same collection of trajectories is shown versus time in Fig. 6. The best fit linear regression of $\log \sigma$ versus $\log t$ gives $\sigma = 1.641 t^{0.504}$ over the range $64 \leqslant t \leqslant 8192$. The slope of the fitted curve (also called the Hurst exponent [29]) indicates that the motion is closely Brownian (for which the slope would be 0.5) with a diffusion coefficient of $D = \sigma^2/t \cong 2.69$. Thus, not only does this system provide a test bed for chaos with an easily and accurately controlled attractor dimension, but it provides an elegant example of Brownian motion from a purely deterministic dynamic.

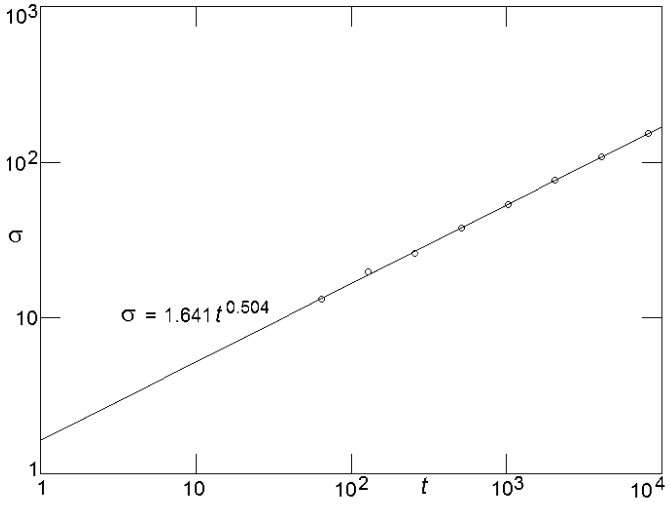

Fig. 6. Standard deviation of 5×10^5 trajectories starting near the origin versus time for $\tau = 20$.

4. Discussion

While the system in Eq. (6) is certainly the simplest DDE with a sinusoidal nonlinearity, there are other simple systems such as

$$\dot{x} = x_\tau - x_\tau^3 \tag{9}$$

for which chaos onsets from a limit cycle at $\tau \cong 1.538$ and persists except for periodic windows until $\tau \cong 1.723$, whereupon the trajectory becomes unbounded with an exponentially growing $x(t)$. Similar behavior is observed with the signs interchanged in Eq. (9) but at a higher value of τ such that the trajectory is unbounded for τ greater than about 3.815. The right-hand side of Eq. (9) can be considered as a scaled version of the first two terms in the Taylor series for $\sin x_\tau$. Other simple polynomial DDEs include the delayed logistic differential equation (also called Hutchinson's equation) [30] $\dot{x} = x - x x_\tau$ used to model single-species population growth [31], and the delayed-action oscillator [32] $\dot{x} = x - x^3 - \alpha x_\tau$ used to model El Niño temperature oscillations in the equatorial Pacific, each of which admits periodic oscillations but apparently not chaos. Thus Eq. (9) may be the simplest chaotic polynomial DDE and is worthy of further study along the lines described here for the sinusoidal case, except that its attractor never exceeds a value of about $D_{KY} \cong 2.3$. These systems are especially amenable to implementation as electrical circuits, where the time delay can be provided by a linear lossless transmission line [33–36].

Acknowledgements

I am grateful to Konstantinos E. Chlouverakis for interesting me in this topic, for stimulating discussions, and confirmation of some of the numerical results, and to George Rowlands for reading the manuscript and offering helpful comments.

References

[1] J.C. Sprott, Phys. Lett. A 228 (1997) 271.
[2] H.P.W. Gottlieb, J.C. Sprott, Phys. Lett. A 291 (2001) 385.
[3] R. Thomas, V. Basios, M. Eiswirth, T. Kruel, O.E. Rössler, Chaos 14 (2005) 669.
[4] J.-M. Malasani, Phys. Lett. A 264 (2000) 383.
[5] S.J. Linz, J.C. Sprott, Phys. Lett. A 259 (1999) 240.
[6] A. Arneodo, P. Coullet, C. Tresser, Phys. Lett. A 79 (1980) 259.
[7] J.A. Vano, J.C. Wildenberg, M.B. Anderson, J.K. Noel, J.C. Sprott, Nonlinearity 19 (2006) 2391.
[8] K.E. Chlouverakis, J.C. Sprott, Chaos Solitons Fractals 28 (2005) 739.
[9] J.C. Sprott, J.C. Wildenberg, Y. Azizi, Chaos Solitons Fractals 26 (2005) 1035.
[10] A. Bellen, M. Zennaro, Numerical Methods for Delay Differential Equations, Oxford Univ. Press, 2003.
[11] Y. Kuang, Delay Differential Equations with Applications in Population Dynamics, Academic Press, San Diego, 1993.
[12] F.R. Sharpe, A.J. Lotka, Am. J. Hygiene 3 (1923) 96.
[13] M. Villasana, A. Radunskaya, J. Math. Biol. 47 (2003) 270.
[14] P.W. Nelson, A.S. Perelson, Math. Biosci. 179 (2002) 73.
[15] R.K. Brayton, Quart. Appl. Math. 24 (1966) 215.
[16] R.D. Driver, J. Differential Equations 54 (1984) 73.
[17] D. Mackey, L. Glass, Science 197 (1977) 28.
[18] J.D. Farmer, Physica D 4 (1982) 366.
[19] P. Grassberger, I. Procaccia, Physica D 13 (1984) 34.
[20] K. Ikeda, K. Matsumoto, Physica D 29 (1987) 223.
[21] K. Ikeda, Opt. Commun. 39 (1979) 257.
[22] A.E. Dubinov, I.D. Dubinova, J. Plasma Phys. 71 (2005) 715.
[23] J.D. Murray, Mathematical Biology, second ed., Springer, New York, 1993.
[24] M.J. Feigenbaum, J. Stat. Phys. 19 (1978) 24.
[25] A. Wolf, J.B. Swift, H.L. Swinney, J.A. Vastano, Physica D 16 (1985) 285.
[26] J. Kaplan, J. Yorke, in: H.-O. Peitgen, H.-O. Walther (Eds.), Functional Differential Equations and Approximations of Fixed Points, in: Lecture Notes in Mathematics, vol. 730, Springer, Berlin, 1979, pp. 228–237.
[27] Ya.B. Pesin, Russian Math. Surv. 32 (1977) 55.
[28] W.H. Press, B.P. Flannery, S.A. Teukolsky, W.T. Vetterling, Numerical Recipes: The Art of Scientific Computing, second ed., Cambridge Univ. Press, 1992.
[29] H.E. Hurst, R.P. Black, Y.M. Simaika, Long-Term Storage: An Experimental Study, Constable, London, 1965.
[30] G.E. Hutchinson, Ann. N.Y. Acad. Sci. 50 (1948) 221.
[31] R.M. May, Stability and Complexity in Model Ecosystems, second ed., Princeton Univ. Press, 1975.
[32] M.J. Suarez, P.S. Schopf, J. Atmos. Sci. 45 (1988) 3283.
[33] G. Mykolaitis, A. Tamaševičius, A. Cenys, S. Bumeliene, A.N. Anagnostopoulos, N. Kalkan, Chaos Solitons Fractals 17 (2003) 343.
[34] A. Namajunas, K. Pyragas, A. Tamaševičius, Int. J. Bifur. Chaos 7 (1997) 957.
[35] A. Namajunas, K. Pyragas, A. Tamaševičius, Phys. Lett. A 201 (1995) 42.
[36] K. Pyragas, A. Tamševičius, Phys. Lett. A 180 (1993) 99.